processes

MDPI

Article

Pinch-Based General Targeting Method for Predicting the Optimal Capital Cost of Heat Exchanger Network

Dianliang Fu [1], Qixuan Li [1], Yan Li [1], Yanhua Lai [1,*], Lin Lu [2,*], Zhen Dong [3] and Mingxin Lyu [1,3]

[1] School of Energy and Power Engineering, Shandong University, Jinan 250061, China
[2] Department of Building Environment and Energy Engineering, The Hong Kong Polytechnic University, Hong Kong, China
[3] Suzhou Research Institute, Shandong University, Suzhou 215123, China
* Correspondence: laiyh@sdu.edu.cn (Y.L.); vivien.lu@polyu.edu.hk (L.L.)

Abstract: Pinch analysis is vital in optimizing heat exchanger networks (HENs). Targeting methods are used when determining cost effectiveness with pinch analysis. However, the existing targeting methods for the capital cost of HEN are not suitable for wide application scenarios. Therefore, we developed a high-accuracy general capital-cost-targeting method. It is built on a final structure that was evolved from the spaghetti structure of HEN through four loop elimination stages. This structure helps to reduce the prediction deviation of the method. To achieve high adaptability while establishing this method, we considered the different heat exchanger cost categories, different cost laws for one stream pair, and area limitations of heat exchangers that may be encountered in practice. In addition, allowing streams to use individual temperature difference contributions enhances the method's predictive capacity. The potential defects of the method found in numerical experiments and case studies were corrected with improvement measures. As a result, the accuracy and stability of the targeting method were further enhanced, with absolute target deviations generally within 10% and often within 5%. This study provides a benchmark for the optimal capital cost of HEN, allowing for a better economic effect when applying pinch analysis.

Keywords: heat exchanger network; pinch analysis; energy recovery; capital cost target; spaghetti structure; general method

Citation: Fu, D.; Li, Q.; Li, Y.; Lai, Y.; Lu, L.; Dong, Z.; Lyu, M. Pinch-Based General Targeting Method for Predicting the Optimal Capital Cost of Heat Exchanger Network. *Processes* **2023**, *11*, 923. https://doi.org/10.3390/pr11030923

Academic Editors: Yimin Zeng and Kaiyang Li

Received: 17 February 2023
Revised: 13 March 2023
Accepted: 15 March 2023
Published: 17 March 2023

1. Introduction

As global energy demands increase and global warming intensifies, the efficient use of energy will continue to be a concern. As one of the effective approaches for process system integration, the optimization of heat exchanger networks (HENs) can fully tap energy-saving potentials to reduce energy waste [1]. The mathematical programming and pinch analysis methods developed for optimizing HEN have long been the subject of many studies. This study aimed to improve the existing methods for calculating the capital cost target of HEN, which has restricted the economy of pinch analysis.

The optimization of HEN is arduous, because the optimal HEN may be hidden in a very large number of possible topology designs [2]. As one class of optimization methods, mathematical programming methods enable the automatic acquisition of the optimal HENs and are continuously progressing via the update of mathematical models and algorithms. To address solution stagnation, Xiao et al. [3] proposed an enhancing strategy promoted by a large step length to advance network structure optimization. Xiao et al. [4] developed this further by adding a strategy of accepting imperfect solutions. An innovative strategy was adopted by Xu et al. [5] to construct viable optimization paths for various issues by combining several modules with various functions. In the effort to improve optimization efficiency, Rathjens and Fieg [6] introduced a hybrid approach of the genetic algorithm (GA) and a strategy based on structure identification and change of reference system (SIR). Feyli et al. [7] combined the GA and the modified quasi-linear programming

(MQLP) model. Unlike the traditional models, Xiao et al. [8] developed a node-dynamic adaptive non-structural model without stream splitting. Nevertheless, pinch analysis is still commonly used because of its interactivity and insight, especially in the field of HEN retrofitting. Regardless of the synthesis or retrofit of HEN, pinch analysis can provide a good optimization interpretation from thermodynamics.

Pinch analysis can provide a clear target for energy recovery and shows strong power in energy saving and utilization. A variety of applications have demonstrated its ability to guide the optimization of HEN. Bayomie et al. [9] achieved additional energy savings for a crude distillation unit by implementing rational process changes. Bandyopadhyay et al. [10] demonstrated how to integrate energy during the design phase of a new plant. For a petroleum refinery's catalyst reforming unit, Wang et al. [11] developed a pinch-based systematic method to guide the integration of various heat pumps. Ghorbani et al. [12] decreased external energy needs for an integrated power generation system. Liu et al. [13] enhanced the profitability of a coal-based methanol to the olefins (MTO) process. Langner et al. [14] used pinch analysis to quantify utility targets and the magnitude of major pinch rule violations in a proposed computational tool to screen retrofit proposals early in the design process. Prior to HEN optimization, the application of pinch analysis needs to determine an optimal target point at the targeting stage by weighing the operating cost target of energy and the capital cost target. Due to the numerous possible HEN structure topologies [15], obtaining a reliable capital cost target [2] is difficult. In reviewing the progress of pinch analysis, Wang et al. [16] concluded that follow-up methods need to be developed to better balance energy savings and capital costs.

Establishing the capital-cost-targeting method with the spaghetti (SPA) structure [17] is the conventional method. Ahmad et al. [18] provided two calculation approaches for capital cost targeting to suit two types of HENs. One type of HEN only uses 1-2 shell and tube heat exchangers, and the other type of HEN is made up of countercurrent heat exchangers. Jegede and Polley [19] found the approach of Ahmad et al. [18] to not be reliable enough. They improved the calculation approach for capital cost targeting for a HEN consisting of countercurrent heat exchangers by using the area and number distributions of matches in the SPA structure under each heat exchanger specification. Serna-González et al. [20] further developed the Jegede and Polley [19] approach, arguing that the individual temperature difference contribution (TDC) of each stream must be optimized based on the difference in heat transfer coefficients of streams to derive better capital cost targeting for HEN.

For a long time afterward, the capital-cost-targeting methods focused on extending previous methods rather than improving accuracy. Akbarnia et al. [21] included a specific pipeline cost in the targeting method. In another study, the capital and operating costs of pumps were considered in the targeting method [22]. The capital-cost-targeting method was also incorporated into an automated targeting model (ATM) framework [23]. Ulyev et al. [24] updated the super targeting procedure by accounting for stream splitting and mixing.

The SPA structure presents vertical heat transfer between streams as the average distribution of heat loads. However, its failure to express the potential for cost reduction by optimizing energy distribution makes the resulting target value often higher than the capital cost of a well-designed optimal HEN. In the work of Fu et al. [25], it is demonstrated that the targeting method based on the SPA structure can cause significant prediction deviations when very different cost laws are used for HEN. To overcome the inherent drawbacks of the SPA structure, Fu et al. [25] used a structure evolved from the spaghetti structure (ESPA structure) for the first time to establish the capital-cost-targeting method, which greatly improved the method's accuracy by considering low-cost matching. Although the ESPA method contributes to improving target accuracy, there is still a risk of the target capital cost being 10% higher than the reference capital cost when HENs adopt very different cost laws. Moreover, the failure to consider the individual stream TDCs limits the predictive capacity of this method. Currently, neither the ESPA method nor the previous targeting methods have yet to consider limiting the maximum areas of heat exchangers, allowing different

cost laws between a pair of heat exchange streams or selecting different cost categories for heat exchangers. As described above, existing targeting methods may be insufficiently accurate or unavailable when facing various application scenarios in practice.

This paper proposes a general method for calculating the capital cost target for HEN, which is lacking in the literature. In addition to inheriting the benefits of using the ESPA structure [25], we further improve the targeting method in three aspects. First, multiple cost categories, different cost laws for one stream pair, and maximum area limitations can be set as needed when obtaining the capital cost target, expanding the applicability range of the method. Second, optimization of individual stream TDCs is allowed, increasing the predictive capacity of the targeting method. Third, further accuracy enhancement strategies are provided to reduce the prediction deviation of the capital cost target to the optimal capital cost. By providing a more powerful target calculation method for the capital cost of HEN, this study contributes to improving the economic benefits and optimization effect of using pinch analysis.

The structure of the paper is as follows. A primary capital-cost-targeting method is first established. Then, the deficiencies of the targeting method are analyzed and corrected using numerical experiments. Based on the targeting method, approaches are suggested for optimizing the stream's uniform or individual TDCs. In case studies, the more appropriate cost target result is chosen to compare with the optimal cost result from the literature, and accuracy enhancement measures are suggested. After that, the technical strengths and limitations of this study are discussed.

2. Problem Statement

In establishing the developed capital cost targeting method, the more comprehensive consideration of the factors affecting the capital cost of heat exchange matching enhances the method's applicability.

2.1. Heat Exchanger Cost Categories

The cost equations presented in the literature for calculating the capital cost CC_U of a heat exchange unit can be classified into two types: one [22] is represented by Equation (1), and the other [18] is represented by Equation (2).

$$CC_U = N_{shell,U}\left[a_l + b_l\left(A_U/N_{shell,U}\right)^{c_l}\right] \tag{1}$$

$$CC_U = a_l + b_l\left(A_U/N_{shell,U}\right)^{c_l} N_{shell,U} \tag{2}$$

The stream flow patterns of heat exchangers in industries can be divided into countercurrent and non-countercurrent [26]. The area ($A_{1-1,U}$) calculation of countercurrent heat exchange unit is shown in Equation (3). The area ($A_{1-2,U}$) of non-countercurrent heat exchange unit is calculated by Equation (4). Here, the 1-2 shell and tube heat exchangers most widely applied in industries are used as the representative of non-countercurrent heat exchangers. The correction factor F_T of logarithmic mean temperature difference (LMTD) is less than one, indicating the reduction of the effective heat transfer temperature difference.

$$A_{1-1,U} = \sum_{x=1}^{X} \frac{q_{U,x}}{\Delta T_{LM,U,x}}\left(\frac{1}{h_{i,U,x}} + \frac{1}{h_{j,U,x}}\right) \tag{3}$$

$$A_{1-2,U} = A_{1-1,U}/F_{T,U} \tag{4}$$

For heat exchangers, there are two types of capital cost equations and two approaches to get the area, which can be combined into four heat exchanger cost categories (HECCs), as shown in Table 1.

Table 1. Four HECCs of HENs.

HECC	Cost Equation	Area Equation
A	Equation (1)	Equation (3)
B	Equation (1)	Equation (4)
C	Equation (2)	Equation (3)
D	Equation (2)	Equation (4)

2.2. Non-Uniform Cost Laws of Heat Exchanger

Usually, a single cost law is adopted for one heat exchanger specification. In special cases, the use of multiple cost laws is necessary [19]. The effect of the stream temperature on the mechanical stress of the heat exchanger construction material is an important reason. Further subdivided cost laws may be required for a heat exchanger specification, see Table 2. Generally, a default cost law, i.e., CL-0 (Default), is used for a heat exchanger specification. The special capital cost calculation due to high temperature is constrained by a cost law such as CL-1 (Hot), and for low temperature, it is governed by a cost law such as CL-2 (Cold).

Table 2. Multiple cost laws are adopted for one heat exchanger specification.

Heat Exchanger Specification	Cost Law	HECC	Temperature Range	Cost Parameters		
l	CL-0 (Default)	A/B/C/D		a_{l-0}	b_{l-0}	c_{l-0}
	CL-1 (Hot)	A/B/C/D	$[T_{min-1}, T_{max-1}]$	a_{l-1}	b_{l-1}	c_{l-1}
	CL-2 (Cold)	A/B/C/D	$[T_{min-2}, T_{max-2}]$	a_{l-2}	b_{l-2}	c_{l-2}
	...	...	...	...	...	...

2.3. Maximum Area Limitation for Heat Exchangers

In practice, heat exchanger size may be constrained by machining capacity, installation requirements, or space. Depending on the situation, the maximum area of the individual shell in the heat exchange unit may need to be limited.

3. General ESPA Method for Capital Cost Target

Figure 1 shows the calculation process of the general ESPA method. The main steps are giving the stream TDCs, generating the shifted balanced composite curves (BCCs) [27], dividing enthalpy intervals, SPA design of enthalpy interval, derivation of the final ESPA structure, and acquisition of the capital cost target.

3.1. Establishment of the SPA Structure

The SPA structure is established by the shifted BCCs rather than the conventional BCCs.

3.1.1. Shifted BCCs

The shifted BCCs (see Figure 1a) are composed of two shifted hot and cold composite curves with equal starting and ending heat loads in the T-Q plot. The pinch occurs where the minimum temperature difference (MTD) between these two curves is zero. Unless otherwise specified, the pinch temperature difference (PTD) refers to the difference between the non-shifted temperatures of a pair of hot and cold streams at the pinch. If streams use individual TDCs, the pinch formed is called diverse pinch [28].

The vertical heat transfer relationship between shifted BCCs determines the heat transfer relationship between streams after removing temperature shifts of stream. When individual TDCs are used for streams, the vertical heat transfer in the shifted BCCs will show cross behavior after removing the temperature shifts of stream. Using the same TDCs for hot and cold streams can be considered a special case of individual TDCs used for streams.

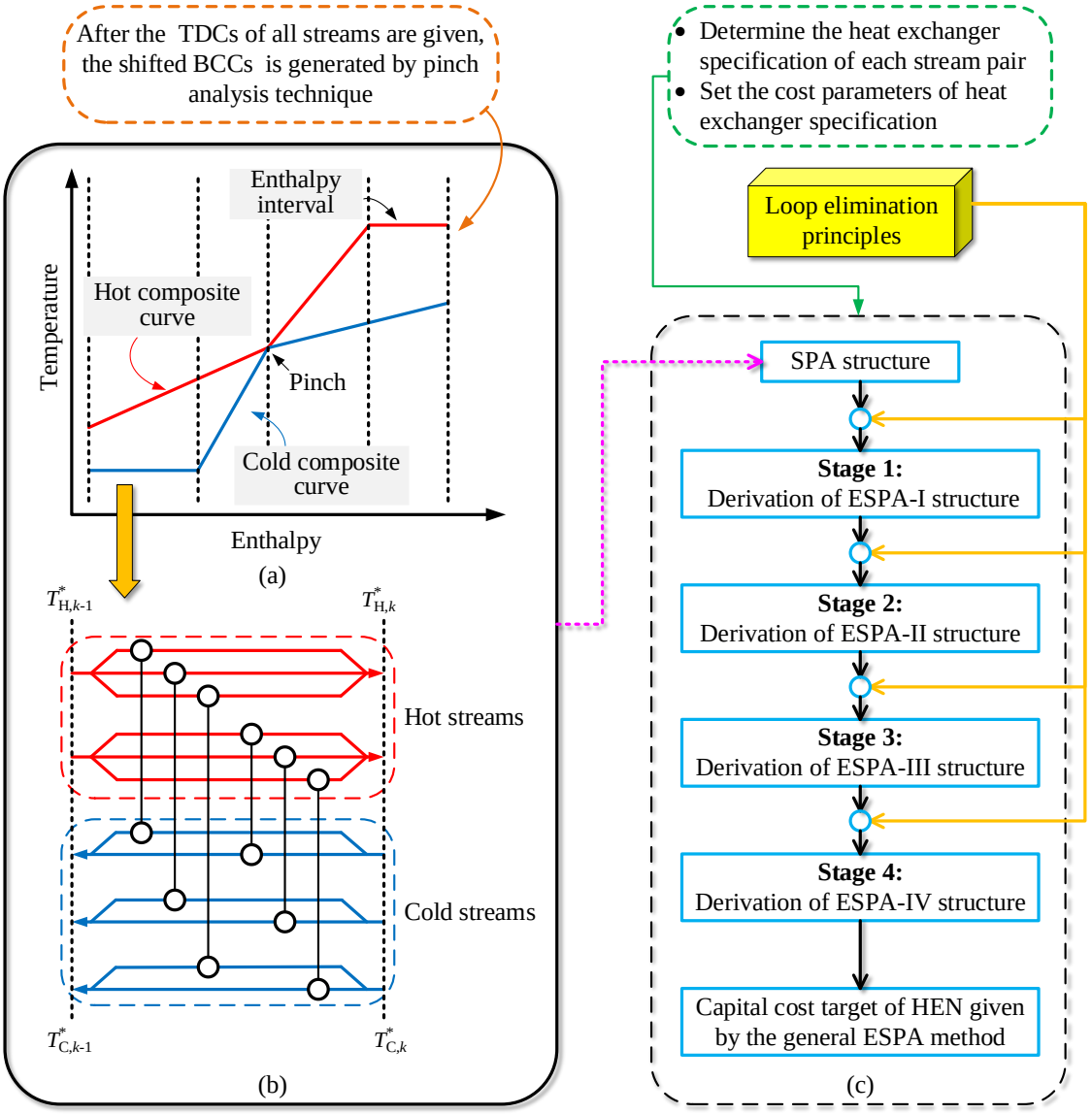

Figure 1. Derivation of the general ESPA method: (**a**) shifted BCCs for the HEN; (**b**) match distribution in enthalpy interval *k* of the SPA structure; (**c**) evolution flowchart of ESPA structures.

3.1.2. Division of Enthalpy Intervals

Obtaining the SPA structure of HEN relies on dividing enthalpy intervals on the shifted BCCs. We expand on Kemp [27] by suggesting enthalpy interval division on the shifted BCCs at each stream's inlet and outlet temperatures and where the stream's property changes. The property may be any of the heat capacity flow rate, heat transfer coefficient, and applicable cost law. The division of enthalpy intervals on the shifted BCCs is shown in Figure 1a.

3.1.3. SPA Structure of HEN

The SPA designs of all enthalpy intervals form the SPA structure of HEN. The SPA design corresponding to enthalpy interval *k* is shown in Figure 1b. The heat load ($q_{m(ij),k}$) between hot stream *i* and cold stream *j* in this enthalpy interval is given by Equation (5). When the flow pattern of the heat exchanger is countercurrent, Equation (6) gives the area ($A_{1-1,m(ij),k}$) of match. If the construction type of 1-2 shell and tube is used for the heat exchanger, the area ($A_{1-2,m(ij),k}$) must be given with additional consideration for F_T, as

shown in Equation (7). The F_T is related to the number of shells in series, N_{shell}, of the match [29]. In order to ensure operational stability, F_T must be at least 0.75.

$$\begin{aligned} q_{m(ij).k} &= \left(CP_{i,k}CP_{j,k} / \sum_{j}^{J} CP_{j,k} \right) \left(T_{i,k-1} - T_{i,k} \right) \\ &= \left(CP_{i,k}CP_{j,k} / \sum_{i}^{I} CP_{i,k} \right) \left(T_{j,k-1} - T_{j,k} \right) \end{aligned} \tag{5}$$

where

$$T_{i,k-1} = T^*_{H,k-1} + \Delta T_{cont,i},\ T_{i,k} = T^*_{H,k} + \Delta T_{cont,i},\ T_{j,k-1} = T^*_{C,k-1} - \Delta T_{cont,j},\ T_{j,k} = T^*_{C,k} - \Delta T_{cont,j}$$

$$A_{1-1,m(ij),k} = \frac{q_{m(ij),k}}{\Delta T_{LM,m(ij),k}} \left(\frac{1}{h_{i,k}} + \frac{1}{h_{j,k}} \right) \tag{6}$$

$$A_{1-2,m(ij),k} = A_{1-1,m(ij),k} / F_{T,m(ij),k} \tag{7}$$

where

$$\Delta T_{LM,m(ij),k} = \left(\Delta T^k_{m(ij)} - \Delta T^{k-1}_{m(ij)} \right) / \ln \left(\Delta T^k_{m(ij)} / \Delta T^{k-1}_{m(ij)} \right),$$

$$\Delta T^k_{m(ij)} = T_{i,k} - T_{j,k},\ \Delta T^{k-1}_{m(ij)} = T_{i,k-1} - T_{j,k-1}$$

3.2. Loop Elimination Principles

The loop is a closed path formed by heat exchange matches [27]. To increase the reliability of the targeting method, the ESPA structure on which the general ESPA method relies will be derived via energy shifts in loops towards low-cost matching, with the SPA structure serving as the initial structure for the evolution. The principles of loop elimination are proposed to guide the energy shift in loops. They address two types of loops: one type is located between the same stream pair and formed with different matches, and the other type is formed by matches among different stream pairs. The former loop is eliminated by merging different matches within this stream pair, reflecting a tendency to reduce redundant and unnecessary heat exchange units in the HEN. For the latter, loop elimination is a nonlinear optimization process. Solving the nonlinear problem is difficult. Here, the loop is eliminated in the following way: confirm the odd and even positions based on the match sequence orders in the loop, and then select the matches with the smallest heat load at the odd and even positions to eliminate. Of the matches in these two locations, the one that minimizes the capital cost will be accepted. The detailed implementation process can be found in Supplementary Material S1.

3.3. Evolution of ESPA Structures

There are four stages to generating ESPA structures, with the final ESPA structure as the foundation for establishing the general ESPA method. The structure evolution is a process of energy aggregation towards low-cost matching until the pinch analysis principles prevent it. The specific performance is that decreasing matches lead to different ESPA structures.

3.3.1. Derivation of the ESPA-I Structure

Loop elimination was first performed in each enthalpy interval of the SPA structure. When there are no loops in enthalpy intervals, the total matching cost is lowest, and the ESPA-I structure, the first evolutionary structure derived from the SPA structure, is obtained.

The capital cost calculations for matches using HECCs A and C are given in Equations (8) and (9). The area of match is the countercurrent heat exchange area. The shell number, $N_{shell,m(ij),k,1-se}$, of a match adopts an average value $N_{shell,ave,m(ij),k,1-se}$. Equations (10) and (11) give

the objective functions to obtain the average number of shells, $N_{\text{shell,ave},m(ij),k,l-se}$, under HECCs A and C.

$$CC_{m(ij),k,l-se} = N_{\text{shell},m(ij),k,l-se}\left(a_{l-se} + b_{l-se}\left(\frac{A_{m(ij),k,l-se}}{N_{\text{shell},m(ij),k,l-se}}\right)^{c_{l-se}}\right), \text{HECC} - \text{A} \in l-se \quad (8)$$

$$CC_{m(ij),k,l-se} = a_{l-se} + b_{l-se}\left(\frac{A_{m(ij),k,l-se}}{N_{\text{shell},m(ij),k,l-se}}\right)^{c_{l-se}} N_{\text{shell},m(ij),k,l-se}, \text{HECC} - \text{C} \in l-se \quad (9)$$

where

$$A_{m(ij),k,l-se} = A_{1-1,m(ij),k},\ N_{\text{shell},m(ij),k,l-se} = N_{\text{shell,ave},m(ij),k,l-se}$$

$$\text{Min } CC_{\text{ave},m(ij),k,l-se} = N_{\text{shell,ave},m(ij),k,l-se}\left(a_{l-se} + b_{l-se}\left(\frac{A_{1-1,\text{ave},m(ij),k,l-se}}{N_{\text{shell,}^{\text{ave}},m(ij),k,l-se}}\right)^{c_{l-se}}\right), \text{HECC} - \text{A} \in l-se \quad (10)$$

$$\text{Min } CC_{\text{ave},m(ij),k,l-se} = a_{l-se} + b_{l-se}\left(\frac{A_{1-1,\text{ave},m(ij),k,l-se}}{N_{\text{shell,}^{\text{ave}},m(ij),k,l-se}}\right)^{c_{l-se}} N_{\text{shell,}^{\text{ave}},m(ij),k,l-se}, \text{HECC} - \text{C} \in l-se \quad (11)$$

where

$$A_{1-1,\text{ave},m(ij),k,l-se} = \frac{q_{\text{ave},m(ij)}}{\Delta T_{\text{LM},m(ij),k}}\left(\frac{1}{h_{i,k}} + \frac{1}{h_{j,k}}\right),$$
$$q_{\text{ave},m(ij)} = \min\left[CP_{i,k}\left(T_{i,k-1} - T_{i,k}\right), CP_{j,k}\left(T_{j,k-1} - T_{j,k}\right)\right]/2$$

Subject,

$$A_{1-1,\text{ave},m(ij),k,l-se}/N_{\text{shell,ave},m(ij),k,l-se} \le A_{\text{limit},l-se},\ N_{\text{shell,ave},m(ij),k,l-se} \in Z+$$

For HECCs B and D, the area of a match is the area of the 1-2 shell and tube heat exchanger on the match. The capital costs of match for these two cost categories are shown in Equations (12) and (13). In the same way as HECCs A and C, the shell number, $N_{\text{shell},m(ij),k,l-se}$, of a match is also equal to the average shell number $N_{\text{shell,ave},m(ij),k,l-se}$. The objective functions to obtain $N_{\text{shell,ave},m(ij),k,l-se}$ are shown in Equations (14) and (15).

$$CC_{m(ij),k,l-se} = N_{\text{shell},m(ij),k,l-se}\left(a_{l-se} + b_{l-se}\left(\frac{A_{m(ij),k,l-se}}{N_{\text{shell},m(ij),k,l-se}}\right)^{c_{l-se}}\right), \text{HECC} - \text{B} \in l-se \quad (12)$$

$$CC_{m(ij),k,l-se} = a_{l-se} + b_{l-se}\left(\frac{A_{m(ij),k,l-se}}{N_{\text{shell},m(ij),k,l-se}}\right)^{c_{l-se}} N_{\text{shell},m(ij),k,l-se}, \text{HECC} - \text{D} \in l-se \quad (13)$$

where

$$A_{m(ij),k,l-se} = A_{1-1,m(ij),k}/F_{\text{T},m(ij),k,l-se},\ F_{\text{T},m(ij),k,l-se} = f_{\text{N\_F}}\left(N_{\text{shell},m(ij),k,l-se}\right),\ N_{\text{shell},m(ij),k,l-se} = N_{\text{shell,ave},m(ij),k,l-se}$$

$$\text{Min } CC_{\text{ave},m(ij),k,l-se} = N_{\text{shell,ave},m(ij),k,l-se}\left(a_{l-se} + b_{l-se}\left(\frac{A_{1-2,\text{ave},m(ij),k,l-se}}{N_{\text{shell,}^{\text{ave}},m(ij),k,l-se}}\right)^{c_{l-se}}\right), \text{HECC} - \text{B} \in l-se \quad (14)$$

$$\text{Min } CC_{\text{ave},m(ij),k,l-se} = a_{l-se} + b_{l-se}\left(\frac{A_{1-2,\text{ave},m(ij),k,l-se}}{N_{\text{shell,}^{\text{ave}},m(ij),k,l-se}}\right)^{c_{l-se}} N_{\text{shell,ave},m(ij),k,l-se}, \text{HECC} - \text{D} \in l-se \quad (15)$$

where

$$A_{1-2,\text{ave},m(ij),k,l-se} = \frac{q_{\text{ave},m(ij)}}{\Delta T_{\text{LM},m(ij),k} F_{\text{T,ave},m(ij),k,l-se}}\left(\frac{1}{h_{i,k}} + \frac{1}{h_{j,k}}\right),$$
$$q_{\text{ave},m(ij)} = \min\left[CP_{i,k}\left(T_{i,k-1} - T_{i,k}\right), CP_{j,k}\left(T_{j,k-1} - T_{j,k}\right)\right]/2,$$
$$F_{\text{T,ave},m(ij),k,l-se} = f_{\text{N\_F}}\left(N_{\text{shell,ave},m(ij),k,l-se}\right)$$

Subject,

$$F_{\text{T,ave},m(ij),k,l-se} \ge 0.75,\ A_{1-2,\text{ave},m(ij),k,l-se}/N_{\text{shell,ave},m(ij),k,l-se} \le A_{\text{limit},l-se},\ N_{\text{shell,ave},m(ij),k,l-se} \in Z+$$

Reducing the number of stream pairs in the ESPA-I structure facilitates low-cost matching by reducing the complexity of HEN, which can be achieved by regulating the retention possibility of the match using a particular stream pair during loop elimination.

This retention possibility of match is reflected by applying appropriate cost reductions to the matches in each enthalpy interval, which is realized by introducing an attraction coefficient (AC) to multiply by the original capital cost, $CC_{m(ij),k,l-se}$, of match. The AC only increases the retention potential for some matches when loops are eliminated. Once the ESPA-I structure is obtained, the capital cost of match is recovered by eliminating the effect of AC. The determination of AC can be found in Supplementary Material S2.

3.3.2. Derivation of the ESPA-II Structure

Loops can be further reduced by merging the matches on the same stream pair in the independent region (above or below the pinch) into one virtual match. The ESPA-II structure is then obtained. Because the merged matches may use different cost laws, the virtual match can be subdivided into several sub-virtual matches with different cost laws.

In the ESPA-II structure, the heat load, $q_{v(ij),ir}$ (Equation (16)), of the virtual match is the sum of the heat loads of its sub-virtual matches. The heat load, $q_{v(ij),ir,l-se}$ (Equation (17)), of the sub-virtual match is a sum of the heat loads of its inner matches that are in the enthalpy intervals of ESPA-I structure. The capital cost, $CC_{v(ij),ir}$ (Equation (18)), of the virtual match is the sum of the capital cost $CC_{v(ij),ir,l-se}$ values of sub-virtual matches. The sub-virtual match as a whole determines its optimal shell number and then gives its expected capital cost.

$$q_{v(ij),ir} = \sum_{se\in l}^{SE} q_{v(ij),ir,l-se} \tag{16}$$

$$q_{v(ij),ir,l-se} = \sum_{z}^{Z} q_{m(ij),z,l-se} \tag{17}$$

$$CC_{v(ij),ir} = \sum_{se\in l}^{SE} CC_{v(ij),ir,l-se} \tag{18}$$

For HECCs A and C, the capital cost, $CC_{v(ij),ir,l-se,}$, of sub-virtual match is obtained after the number of shells, $N_{\text{shell},v(ij),ir,l-se,}$ is optimized. The objective functions for optimization are given in Equations (19) and (20).

$$\text{Min } CC_{v(ij),ir,l-se} = N_{\text{shell},v(ij),ir,l-se}\left(a_{l-se} + b_{l-se}\left(\frac{A_{v(ij),ir,l-se}}{N_{\text{shell},v(ij),ir,l-se}}\right)^{c_{l-se}}\right), \text{HECC} - \text{A} \in l - se \tag{19}$$

$$\text{Min } CC_{v(ij),ir,l-se} = a_{l-se} + b_{l-se}\left(\frac{A_{v(ij),ir,l-se}}{N_{\text{shell},v(ij),ir,l-se}}\right)^{c_{l-se}} N_{\text{shell},v(ij),ir,l-se}, \text{HECC} - \text{C} \in l - se \tag{20}$$

where

$$A_{v(ij),ir,l-se} = \sum_{z=1}^{Z} A_{1-1,m(ij),z,l-se},\ A_{1-1,m(ij),z,l-se} = f_{\text{q\_A1}-1}\left(q_{m(ij),z,l-se}\right)$$

Subject,

$$A_{v(ij),ir,l-se}/N_{\text{shell},v(ij),ir,l-se} \le A_{\text{limit},l-se},\ N_{\text{shell},v(ij),ir,l-se} \in Z+$$

For HECCs B and D, two objective functions used to give the optimal number of shells of sub-virtual match are shown in Equations (21) and (22).

$$\text{Min } CC_{v(ij),ir,l-se} = N_{\text{shell},v(ij),ir,l-se}\left(a_{l-se} + b_{l-se}\left(\frac{A_{v(ij),ir,l-se}}{N_{\text{shell},v(ij),ir,l-se}}\right)^{c_{l-se}}\right), \text{HECC} - \text{B} \in l - se \tag{21}$$

$$\text{Min } CC_{v(ij),ir,l-se} = a_{l-se} + b_{l-se}\left(\frac{A_{v(ij),ir,l-se}}{N_{\text{shell},v(ij),ir,l-se}}\right)^{c_{l-se}} N_{\text{shell},v(ij),ir,l-se}, \text{HECC} - \text{D} \in l - se \tag{22}$$

where

$$A_{v(ij),ir,l-se} = \sum_{z}^{Z} \frac{A_{1-1,m(ij),z,l-se}}{F_{\mathrm{T},m(ij),z,l-se}},\ A_{1-1,m(ij),z,l-se} = f_{\mathrm{q\_A1-1}}\left(q_{m(ij),z,l-se}\right),$$
$$F_{\mathrm{T},m(ij),z,l-se} = f_{\mathrm{N\_F}}\left(N_{\mathrm{shell},m(ij),z,l-se}\right),\ N_{\mathrm{shell},m(ij),z,l-se} = RT_{N(\mathrm{ESPA-I}),m(ij),z,l-se} N_{\mathrm{shell},v(ij),ir,l-se}$$

Subject,

$$A_{v(ij),ir,l-se} / N_{\mathrm{shell},v(ij),ir,l-se} \le A_{\mathrm{limit},l-se},\ N_{\mathrm{shell},v(ij),ir,l-se} \in Z+,$$
$$N_{\mathrm{shell},v(ij),ir,l-se} \ge \left(N_{shell,v(ij),ir,l-se}\right)_{\mathrm{ESPA-I,refer}}$$

As seen from Equation (23), $RT_{N(\mathrm{ESPA-I}),m(ij),z,l-se}$ is the ratio of the reference shell number of $N_{\mathrm{shell},m(ij),ir,l-se}$ of the match merged into the sub-virtual match to the reference overall shell number of $N_{\mathrm{shell},v(ij),ir,l-se}$ (see Equation (24)) of the sub-virtual match.

$$RT_{N(\mathrm{ESPA-I}),m(ij),z,l-se} = \frac{\left(N_{\mathrm{shell},m(ij),z,l-se}\right)_{\mathrm{ESPA-I,refer}}}{\left(N_{\mathrm{shell},v(ij),ir,l-se}\right)_{\mathrm{ESPA-I,refer}}} \tag{23}$$

$$\left(N_{\mathrm{shell},v(ij),ir,l-se}\right)_{\mathrm{ESPA-I,refer}} = \sum_{z}^{Z}\left(N_{\mathrm{shell},m(ij),z,l-se}\right)_{\mathrm{ESPA-I,refer}} \tag{24}$$

The reference shell number of $N_{\mathrm{shell},m(ij),ir,l-se}$ is the optimal shell number for the match in the enthalpy interval of ESPA-I structure when the area is unconstrained but needs to make the $F_{\mathrm{T},m(ij),z,l-se}$ not less than 0.75. The objective functions for HECCs B and D to obtain the reference shell number of $N_{\mathrm{shell},m(ij),ir,l-se}$ are given in Equations (25) and (26).

$$\mathrm{Min}\ CC_{m(ij),z,l-se} = N_{\mathrm{shell},m(ij),z,l-se}\left(a_{l-se} + b_{l-se}\left(\frac{A_{m(ij),z,l-se}}{N_{\mathrm{shell},m(ij),z,l-se}}\right)^{c_{l-se}}\right), \mathrm{HECC-B} \in l-se \tag{25}$$

$$\mathrm{Min}\ CC_{m(ij),z,l-se} = a_{l-se} + b_{l-se}\left(\frac{A_{m(ij),z,l-se}}{N_{\mathrm{shell},m(ij),z,l-se}}\right)^{c_{l-se}} N_{\mathrm{shell},m(ij),z,l-se}, \mathrm{HECC-D} \in l-se \tag{26}$$

where

$$A_{m(ij),z,l-se} = A_{1-1,m(ij),z,l-se} / F_{\mathrm{T},m(ij),z,l-se},\ A_{1-1,m(ij),z,l-se} = f_{\mathrm{q\_A1-1}}\left(q_{m(ij),z,l-se}\right),$$
$$F_{\mathrm{T},m,m(ij),z,l-se} = f_{\mathrm{N\_F}}\left(N_{\mathrm{shell},m(ij),z,l-se}\right)$$

Subject,

$$F_{\mathrm{T},m(ij),z,l-se} \ge 0.75,\ N_{\mathrm{shell},m(ij),z,l-se} > 0$$

3.3.3. Derivation of the ESPA-III Structure

The virtual matches in each independent region of ESPA-II structure may form loops. By eliminating loops formed by these virtual matches, the ESPA-II structure was further evolved into the ESPA-III structure. Application of the loop elimination principles required the capital cost, $CC_{v(ij),ir}$, of the virtual match in the independent region. During the evolution from the ESPA-II structure to the ESPA-III structure, the $CC_{v(ij),ir}$ was the sum of the capital cost $CC_{v(ij),ir,l-se}$ values of sub-virtual matches, see Equation (27).

$$CC_{v(ij),ir} = \sum_{se \in l}^{SE} CC_{v(ij),ir,l-se} \tag{27}$$

For various HECCs, the values of the capital cost $CC_{v(ij),ir,l-se}$ of sub-virtual match are given by Equations (28) and (29). The shell number, $N_{\mathrm{shell},v(ij),ir,l-se}$, for the sub-virtual match is the sum of shell numbers of its inner implied matches located in enthalpy intervals.

The $N_{\text{shell},m(ij),z,l-se}$, $\Delta T_{\text{LM},m(ij),z,l-se}$, and $F_{\text{T},m(ij),z,l-se}$ of the inner implied match are treated as fixed expected values when energy is shifted in the loop to form the ESPA-III structure.

If HECC − Aor B ∈ $l - se$,

$$CC_{v(ij),ir,l-se} = \begin{cases} N_{\text{shell},v(ij),ir,l-se}\left(a_{l-se} + b_{l-se}\left(\frac{A_{v(ij),ir,l-se}}{N_{\text{shell},v(ij),ir,l-se}}\right)^{c_{l-se}}\right), if\ A_{v(ij),ir,l-se} \neq 0 \\ 0, \text{ if } A_{v(ij),ir,l-se} = 0 \end{cases} \quad (28)$$

If HECC − Cor D ∈ $l - se$,

$$CC_{v(ij),ir,l-se} = \begin{cases} a_{l-se} + b_{l-se}\left(\frac{A_{v(ij),ir,l-se}}{N_{\text{shell},v(ij),ir,l-se}}\right)^{c_{s-se}} N_{\text{shell},v(ij),ir,l-se}, if\ A_{v(ij),ir,l-se} \neq 0 \\ 0, \text{ if } A_{v(ij),ir,l-se} = 0 \end{cases} \quad (29)$$

where

$$A_{v(ij),ir,l-se} = \begin{cases} \sum_{z}^{Z} \frac{q_{m(ij),z,l-se}}{\Delta T_{\text{LM},m(ij),z,l-se}}\left(\frac{1}{h_{i,z}} + \frac{1}{h_{j,z}}\right), \text{ HECC} - \text{Aor C} \in l - se \\ \sum_{z}^{Z} \frac{q_{m(ij),z,l-se}}{\Delta T_{\text{LM},m(ij),z,l-se} F_{\text{T},m(ij),z,l-se}}\left(\frac{1}{h_{i,z}} + \frac{1}{h_{j,z}}\right), \text{ HECC} - \text{Bor D} \in l - se \end{cases},$$

$$q_{m(ij),z,l-se} = RT_{q(\text{ESPA}-\text{II}),m(ij),z,l-se} q_{v(ij),ir},\ RT_{q(\text{ESPA}-\text{II}),m(ij),z,l-se} = \frac{\left(q_{m(ij),z,l-se}\right)_{\text{ESPA}-\text{II,refer}}}{\left(q_{v(ij),ir}\right)_{\text{ESPA}-\text{II,refer}}},$$

$$\left(q_{v(ij),ir}\right)_{\text{ESPA}-\text{II,refer}} = \sum_{z}^{Z}\left(q_{m(ij),z,l-se}\right)_{\text{ESPA}-\text{II,refer}}$$

It is worth noting that the matches within the enthalpy interval are in parallel. We assumed that multiple matches were on a stream and that one had an especially high matching cost due to its special heat transfer coefficient or cost law. It would have been a serious violation of cost optimization behavior to keep the parallel relationship for these matches. A solution was adopted to change the location relationship of these matches from parallel to serial, making the high-cost or low-cost matching use a larger or smaller temperature difference. The change of matches in the enthalpy interval corrected the capital cost calculation of the virtual match in the ESPA-III structure. The change criteria for match locations from parallel to serial rely on two parameters $RT_{CC,v(ij),wr}$ and $RT_{cc(\text{A}),v(ij),wr}$, as detailed in Supplementary Material S3.

3.3.4. Derivation of the ESPA-IV Structure

After obtaining the ESPA-III structure, the virtual matches between the same stream pair in different independent regions above and below the pinch could be merged to reduce loops further, and the ESPA-IV structure was formed. Further loop elimination would have resulted in heat transfer across the pinch, which is not permitted by pinch analysis.

In the ESPA-IV structure, the heat load, $q_{v(ij),wr}$ (Equation (30)), of the virtual match is the sum of the heat loads of its sub-virtual matches. The heat load, $q_{v(ij),wr,l-se}$ (Equation (31)), of sub-virtual match can be subdivided into different values of the heat load, $q_{m(ij),z,l-se}$, of its corresponding match located in the enthalpy interval of the ESPA-IV structure. The capital cost, $CC_{v(ij),wr}$ (Equation (32)), of the virtual match is the sum of all values of the capital cost, $CC_{v(ij),wr,l-se}$, of its sub-virtual match. The capital cost of sub-virtual match is obtained by taking the shell number of sub-virtual as a whole to optimize, which can be treated as an expected capital cost.

$$q_{v(ij),wr} = \sum_{se \in l}^{SE} q_{v(ij),wr,l-se} \quad (30)$$

$$q_{v(ij),wr,l-se} = \sum_{z}^{Z} q_{m(ij),z,l-se} \quad (31)$$

$$CC_{v(ij),wr} = \sum_{se \in l}^{SE} CC_{v(ij),wr,l-se} \quad (32)$$

The HECCs A and C use the area calculation of countercurrent heat exchanger. For these two HECCs, the objective functions for optimizing the shell number, $N_{\text{shell},v(ij),wr,l-se}$, of sub-virtual matching are shown in Equations (33) and (34).

$$\text{Min } CC_{v(ij),wr,l-se} = N_{\text{shell},v(ij),wr,l-se}\left(a_{l-se} + b_{l-se}\left(\frac{A_{v(ij),wr,l-se}}{N_{\text{shell},v(ij),wr,l-se}}\right)^{c_{l-se}}\right), \text{HECC} - \text{A} \in l - se \quad (33)$$

$$\text{Min } CC_{v(ij),wr,l-se} = a_{l-se} + b_{l-se}\left(\frac{A_{v(ij),wr,l-se}}{N_{\text{shell},v(ij),wr,l-se}}\right)^{c_{l-se}} N_{\text{shell},v(ij),wr,l-se}, \text{HECC} - \text{C} \in l - se \quad (34)$$

where

$$A_{v(ij),wr,l-se} = \sum_{z}^{Z} A_{1-1,m(ij),z,l-se},\ A_{1-1,m(ij),z,l-se} = f_{\text{q\_A1}-1}\left(q_{m(ij),z,l-se}\right)$$

Subject,

$$A_{v(ij),wr,l-se}/N_{\text{shell},v(ij),wr,l-se} \le A_{\text{limit},l-se},\ N_{\text{shell},v(ij),wr,l-se} \in Z+$$

For HECCs B and D that use the area calculation of 1-2 shell and tube heat exchanger, Equations (35) and (36) give two objective functions for optimizing the shell number, $N_{\text{shell},v(ij),wr,l-se}$, of sub-virtual match.

$$\text{Min } CC_{v(ij),wr,l-se} = N_{\text{shell},v(ij),wr,l-se}\left(a_{l-se} + b_{l-se}\left(\frac{A_{v(ij),wr,l-se}}{N_{\text{shell},v(ij),wr,l-se}}\right)^{c_{l-se}}\right), \text{HECC} - \text{B} \in l - se \quad (35)$$

$$\text{Min } CC_{v(ij),wr,l-se} = a_{l-se} + b_{l-se}\left(\frac{A_{v(ij),wr,l-se}}{N_{\text{shell},v(ij),wr,l-se}}\right)^{c_{l-se}} N_{\text{shell},v(ij),wr,l-se}, \text{HECC} - \text{D} \in l - se \quad (36)$$

where

$$A_{v(ij),wr,l-se} = \sum_{z}^{Z} \frac{A_{1-1,m(ij),z,l-se}}{F_{T,m(ij),z,l-se}},\ A_{1-1,m(ij),z,l-se} = f_{\text{q\_A1}-1}\left(q_{m(ij),z,l-se}\right),$$
$$F_{T,m,m(ij),z,l-se} = f_{N\_F}\left(N_{\text{shell},m(ij),z,l-se}\right),\ N_{\text{shell},m(ij),z,l-se} = RT_{N(\text{ESPA}-III),m(ij),z,l-se} N_{\text{shell},v(ij),wr,l-se}$$

Subject,

$$A_{v(ij),wr,l-se}/N_{\text{shell},v(ij),wr,l-se} \le A_{\text{limit},l-se},\ N_{\text{shell},v(ij),wr,l-se} \in Z+,$$
$$N_{\text{shell},v(ij),wr,l-se} \ge \left(N_{\text{shell},v(ij),wr,l-se}\right)_{\text{ESPA}-III,\text{refer}}$$

As shown in Equation (37), $RT_{N(\text{ESPA}-\text{III}),m(ij),z,l-se}$ is the ratio of the reference shell number of $N_{\text{shell},m(ij),ir,l-se}$ for the match in the enthalpy interval of ESPA-III structure to the reference shell number of $N_{\text{shell},v(ij),wr,l-se}$ (see Equation (38)) for its corresponding sub-virtual match.

$$RT_{N(\text{ESPA}-\text{III}),m(ij),z,l-se} = \frac{\left(N_{\text{shell},m(ij),z,l-se}\right)_{\text{ESPA}-\text{III,refer}}}{\left(N_{\text{shell},v(ij),wr,l-se}\right)_{\text{ESPA}-\text{III,refer}}} \quad (37)$$

$$\left(N_{\text{shell},v(ij),wr,l-se}\right)_{\text{ESPA}-\text{III,refer}} = \sum_{z}^{Z}\left(N_{\text{shell},m(ij),z,l-se}\right)_{\text{ESPA}-\text{III,refer}} \quad (38)$$

The reference shell number of $N_{\text{shell},m(ij),ir,l-se}$ is the optimal shell number for the match in the enthalpy interval of ESPA-III structure. The objective functions for HECCs B and D to obtain the reference shell number of $N_{\text{shell},m(ij),ir,l-se}$ are given in Equations (39) and (40).

$$\text{Min } CC_{m(ij),z,l-se} = N_{\text{shell},m(ij),z,l-se}\left(a_{l-se} + b_{l-se}\left(\frac{A_{m(ij),z,l-se}}{N_{\text{shell},m(ij),z,l-se}}\right)^{c_{l-se}}\right), \text{HECC} - \text{B} \in l - se \quad (39)$$

$$\text{Min } CC_{m(ij),z,l-se} = a_{l-se} + b_{l-se}\left(\frac{A_{m(ij),z,l-se}}{N_{\text{shell},m(ij),z,l-se}}\right)^{c_{l-se}} N_{\text{shell},m(ij),z,l-se}, \text{HECC} - \text{D} \in l - se \quad (40)$$

where

$$A_{m(ij),z,l-se} = A_{1-1,m(ij),z,l-se}/F_{\text{T},m(ij),z,l-se},\ A_{1-1,m(ij),z,l-se} = f_{\text{q\_A1}-1}\left(q_{m(ij),z,l-se}\right),$$
$$F_{\text{T},m(ij),z,l-se} = f_{\text{N\_F}}\left(N_{\text{shell},m(ij),z,l-se}\right)$$

Subject,

$$F_{\text{T},m(ij),z,l-se} \geq 0.75,\ N_{\text{shell},m(ij),z,l-se} > 0$$

3.4. Target Value of Capital Cost for HEN

The capital cost target, CC_{TC}, of HEN is the sum of the capital costs of the virtual matches of ESPA-IV structure, see Equation (41). The distribution of virtual matches in the ESPA-IV structure can represent an expected distribution of matches for the HEN. The total capital cost of these virtual matches can be used to predict the optimal capital cost of HEN.

$$CC_{\text{TC}} = \sum_{v}^{V} CC_{v(ij),wr} \quad (41)$$

4. Accuracy Test and Analysis of General ESPA Method

Numerical experiments tested the accuracy of the established general ESPA method. According to test results, the deficiencies in the method establishment process were analyzed and corrected to improve the accuracy of the targeting method further.

4.1. Accuracy Evaluation

The accuracy of the proposed capital cost targeting method was evaluated by using the target deviation $D_{\text{T/R}}$ (see Equation (42)) as an indication. Positive or negative $D_{\text{T/R}}$ meant that the capital cost target, CC_{TC}, of HEN, given by the general ESPA method, was higher or lower than the provided reference capital cost CC_{RC} that represents the optimal capital cost of HEN. The closer the deviation $D_{\text{T/R}}$ was to zero, the more accurate the general ESPA method was.

$$D_{\text{T/R}} = \left(\frac{CC_{\text{TC}}}{CC_{\text{RC}}} - 1\right) \times 100\% \quad (42)$$

4.2. Accuracy Test of General ESPA Method

The stability and accuracy of the general ESPA method were tested under uniform TDCs for hot and cold streams. The HEN example used comes from Ref. [30]. Three types of numerical experiments were provided to test the general accuracy of method. Numerical experiment 1 tested the accuracy when there was no apparent matching preference between streams. In numerical experiment 2, there was a significant difference in heat exchanger specifications or stream heat transfer coefficients. Numerical experiment 3 was special: different cost laws were used by one heat exchanger specification. The capital cost targets for any HECC with and without the maximum area limitations were provided for each case of numerical experiments. When the area constraint was imposed, the maximum area of a single shell was set as 250 m^2, which is suitable for triggering the significant increase in shell number. The specific numerical experimental design is shown in Supplementary Material S4. S4 also provides the optimal HEN structures (see Figure S2) for the cases of numerical experiments. Fu et al. [25] confirmed their thermodynamic rationality. Based on these structures, the optimal capital costs of HENs, i.e., the reference capital costs, were obtained to evaluate the target deviation of the targeting method.

The capital cost target deviations for various cases in the three types of numerical experiments are shown in Figure 2. The target deviation range of all numerical experiments was (−10.3%, 13.5%), with a maximum deviation amplitude of 23.8%. The absolute target

deviations were basically controlled within 10%, except for several positive target deviations of nearly 15%. Even though multiple cost laws are used for a heat exchanger specification, the capital cost targets provided by the general ESPA method have excellent accuracy. However, two problems require attention. One is that individual cases enlarged the amplitude of that target deviation, such as cases 8 and 4, which are in the second and third numerical experiments, respectively. The other is that the overall deviation of test cases was negative.

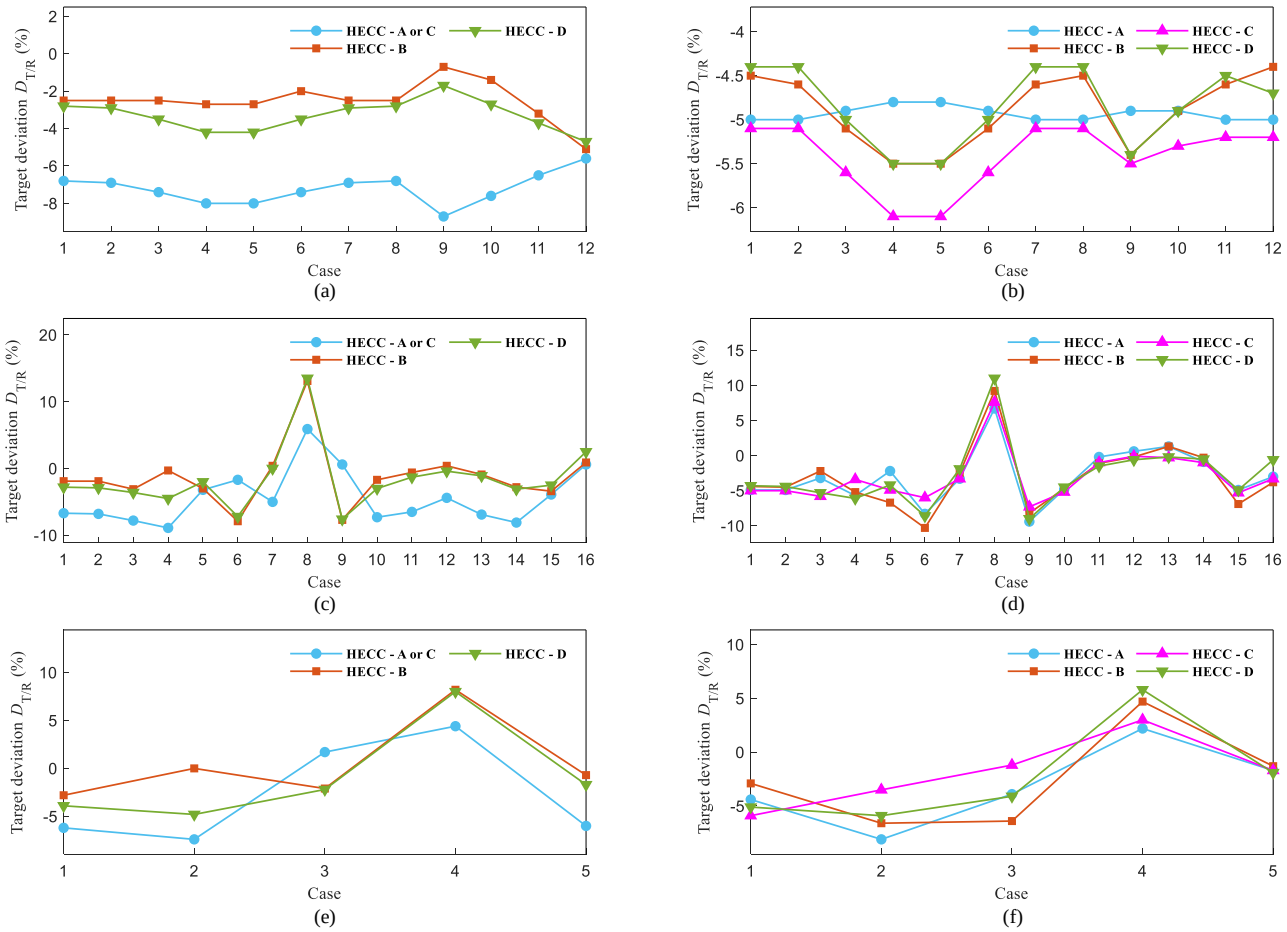

Figure 2. Target deviations for cases in three types of numerical experiments: (**a**,**b**) cases for the first type without and with maximum area limitations; (**c**,**d**) cases for the second type without and with maximum area limitations; (**e**,**f**) cases for the third type without and with maximum area limitations.

4.3. Analysis and Improvement of the General ESPA Method

The deviation amplitude reduction is addressed first, and then a measure is suggested to make the target deviation tend to zero.

4.3.1. Measure for Enhancing Stability

The poor stability of target deviation was mainly caused by target deviations of 13.5% and 8.2%, which occurred in case 8 of the second numerical experiment and case 4 of the third numerical experiment. By adjusting criteria to make the parameter $RT_{cc(\mathrm{A}),v(ij),wr}$ greater than 2.5 to trigger a parallel-to-serial operation, the target deviations' stability improved. The results of the target deviation are shown in Figure 3. The largest positive target deviations for two problem cases were remedied, while the other cases were basically unaffected. At this point, the target deviation range of all cases was (−10.3%, 2.5%) with a maximum deviation amplitude of 12.8%, verifying the effectiveness of the stability measure.

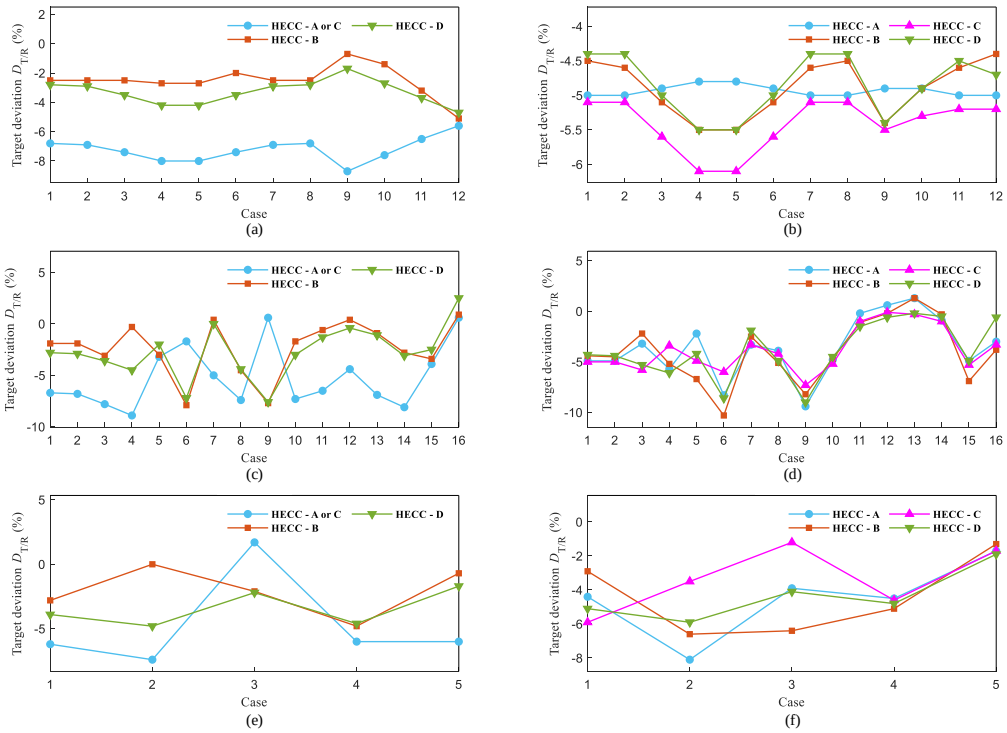

Figure 3. By adopting the stability measure, the target deviations for cases in three types of numerical experiments were as shown above: (**a**,**b**) contains cases for the first type without and with maximum area limitations; (**c**,**d**) contains cases for the second type without and with maximum area limitations; (**e**,**f**) contains cases for the third type without and with maximum area limitations.

4.3.2. Measure for Improving Accuracy

The problem of over-optimizing, which makes the capital cost target too small, needed to be solved. When the ESPA-II structure evolves into the ESPA-III structure, the virtual match adopts the temporary value of $(cc_{v(ij),ir})_{\text{shifted}}$, that is, the product of its original capital cost $(cc_{v(ij),ir})_{\text{shifted}}$ and the γ power of its energy shift ratio (ESR); see Equation (43). The $ESR_{v(ij),ir}$ is the ratio of the energy of a virtual match in the process of loop elimination to its initial value given in the ESPA-II structure. The larger the ESR, the larger the temporary capital cost of the virtual match, which restrains the excessive energy shift towards low-cost matching. The exponent γ can adjust the degree of restraint for the energy shift.

$$\left(cc_{v(ij),ir}\right)_{\text{shifted,temp}} = \left(cc_{v(ij),ir}\right)_{\text{shifted}} \left(ESR_{v(ij),ir}\right)^{\gamma} \tag{43}$$

where

$$ESR_{v(ij),ir} = \frac{\left(q_{v(ij),ir}\right)_{\text{shifted}}}{\left(q_{v(ij),ir}\right)_{\text{ESPA}-\text{II}}}$$

The average of the target deviations under four HECCs is provided for each numerical experiment, with an ESR exponent γ of 1, 2, or 3 (see Figure 4). For the exponents of ESR with 1, 2, and 3, the non-average target deviation under each HECC can be seen in Figures S3–S5, respectively. Here, the average of the capital targets under values of 1 and 3 for γ is used as the capital cost target of HEN. Not only does the target deviation perform a bit better, but the way of averaging is also beneficial to increase the stability of calculation. After the accuracy measure, the target deviations for all test cases were as shown in Figure 5. The target deviation was controlled within the range of $(-7.4\%, 5.7\%)$ with a maximum deviation amplitude of 13.1%. Now, the obtained capital cost target can have a considerable

degree of accuracy and stability to predict the optimal capital cost of HEN and present good applicability to various working conditions.

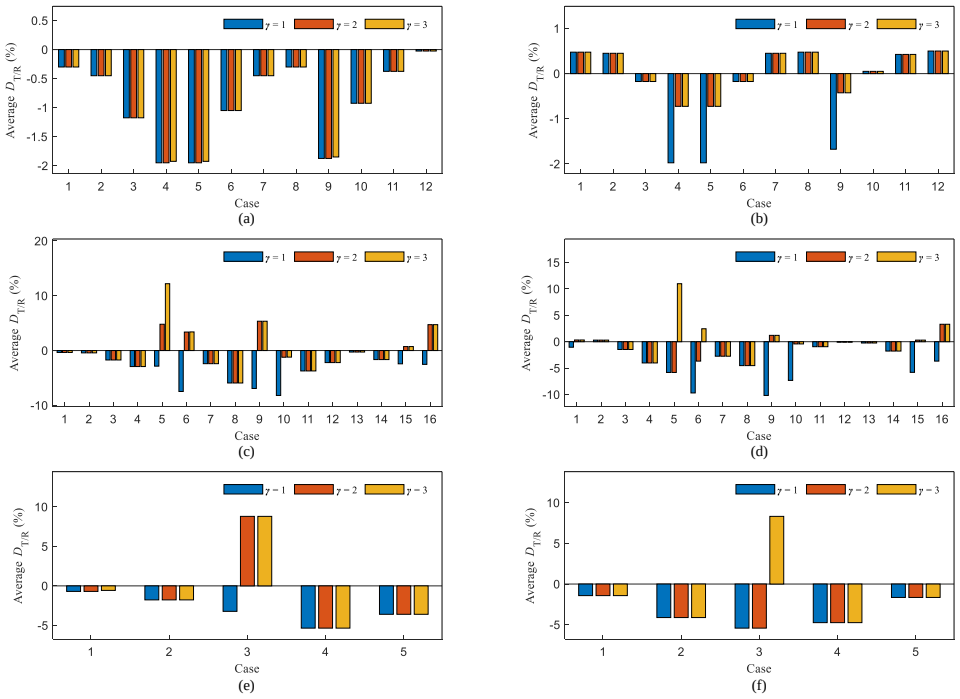

Figure 4. Given an exponent γ of ESR = 1, 2, or 3, the average target deviations for cases in three types of numerical experiments were as shown above; (**a**,**b**) contains cases for the first type without and with maximum area limitations; (**c**,**d**) contains cases for the second type without and with maximum area limitations; (**e**,**f**) contains cases for the third type without and with maximum area limitations.

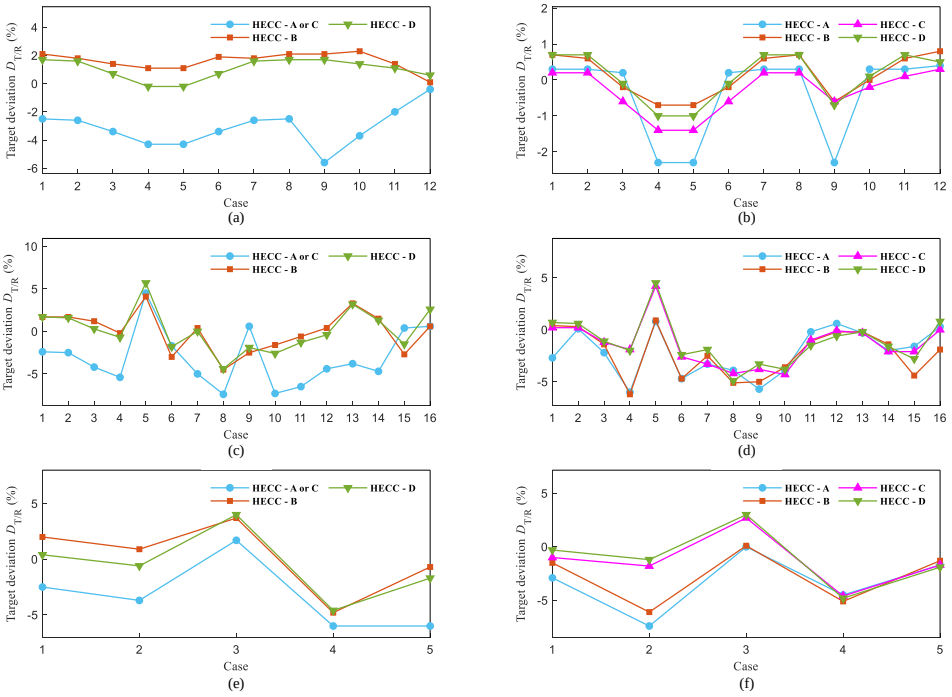

Figure 5. By adopting the accuracy measure, the target deviations for cases in three types of numerical experiments were as shown above; (**a**,**b**) contains cases for the first type without and with maximum area limitations; (**c**,**d**) contains cases for the second type without and with maximum area limitations; (**e**,**f**) contains cases for the third type without and with maximum area limitations.

5. Optimization of the TDCs of Stream

By optimizing the TDCs of stream, a pinch analysis with cost-effective target values could be obtained, which is a good start for applying pinch analysis.

5.1. Uniform TDCs for Streams

When using uniform TDCs for streams, the PTD between BCCs is the sum of two TDCs from hot and cold streams. The operating cost target and capital cost target change as the PTD changes. It is simple to find the optimal PTD with the lowest total annual cost target. Because of this concise and clear correspondence relationship, uniform TDCs of hot and cold streams are widely used for pinch analysis.

5.2. Individual TDCs for Streams

Optimizing the individual TDCs of stream so that pinch analysis has a high economy is more complex. One set of individual TDCs of stream corresponds to an operating cost target and a capital cost target that can be determined, respectively, using pinch analysis and the general ESPA method. The best economic trade-off for these two targets is hidden in various sets of individual stream TDCs. Stochastic optimization methods based on a global search mechanism [8] can be used to optimize the individual TDC of each stream. Single-objective optimization is commonly used. If necessary, multi-objective optimization can be adopted to obtain the Pareto frontier solution set [31].

6. Case Studies

The comparison of the target cost results and the optimal cost results from the literature are presented to verify the reliability of the proposed general ESPA method. Four case studies that took into account the different sizes of HEN, different HECCs, and whether there were maximum area limitations were involved. The optimal capital cost targets or total annual cost targets for HENs with both uniform and individual TDCs of stream were provided for selection.

6.1. Case Study 1

In this case [32], the HEN consisted of 1-2 shell and tube heat exchangers, and the HECC was type B. The HEN was a problem of six streams. Galli and Cerdá [32] developed a mixed-integer linear programming problem formulation that yielded optimal capital costs of $263,854 and $267,747 for the HEN without and with maximum area limitation (50 ft^2) at a fixed 292 Btu/h of the hot utility. These two capital cost values could be used to evaluate the obtained optimal capital cost targets. The case data and the process of obtaining the target value for comparison with the reference cost can be found in Supplementary Material S6.1. HEN optimization is a threshold problem [33] due to the constant usage of utility in the given PTD range under uniform stream TDCs. The target value obtained by optimizing the TDCs of the stream is given in case 1 of Table 3.

Table 3. Predictive accuracy of the optimal target value for each case.

Case	Optimal Cost	Uniform TDCs		Individual TDCs		A_{max} Limitation	Location
		Cost Target	Cost Deviation	Cost Target	Cost Deviation		
1 (a)	263,854 $	262,510 $	/	241,131 $	−8.61%	No	Figure 6a
1 (b)	267,747 $	267,054 $	/	251,503 $	−6.07%	Yes	Figure 6b
2	1,517,678 $/y	1,500,795 $/y	−1.1%	1,458,096 $/y	/	No	Figure 6c
3	6,712,551 $/y	6,607,394 $/y	/	6,476,863 $/y	−3.5%	No	Figure 6d
4	1,852,723 $/y	1,864,328 $/y	/	1,803,354 $/y	−2.7%	No	Figure 6e

Without maximum area limitation for HEN, the target deviations of capital cost using optimal uniform and individual TDCs of stream were −0.51% and −8.61%, respectively. If there was a maximum area limitation, the target deviations of capital cost were −0.26% and −6.07%, respectively. The results show that the target value under optimal uniform

TDCs is better. However, since Galli and Cerdá [32] did not constrain the streams to use a common MTD in their optimization method, the capital cost target deviations of −8.61% and −6.07% under optimal individual TDCs of streams needed to be adopted for the scenarios without and with maximum area limitations. The absolute target deviation of capital cost was controlled within 10%, but the capital cost target deviation of −8.61% is fairly close to −10%.

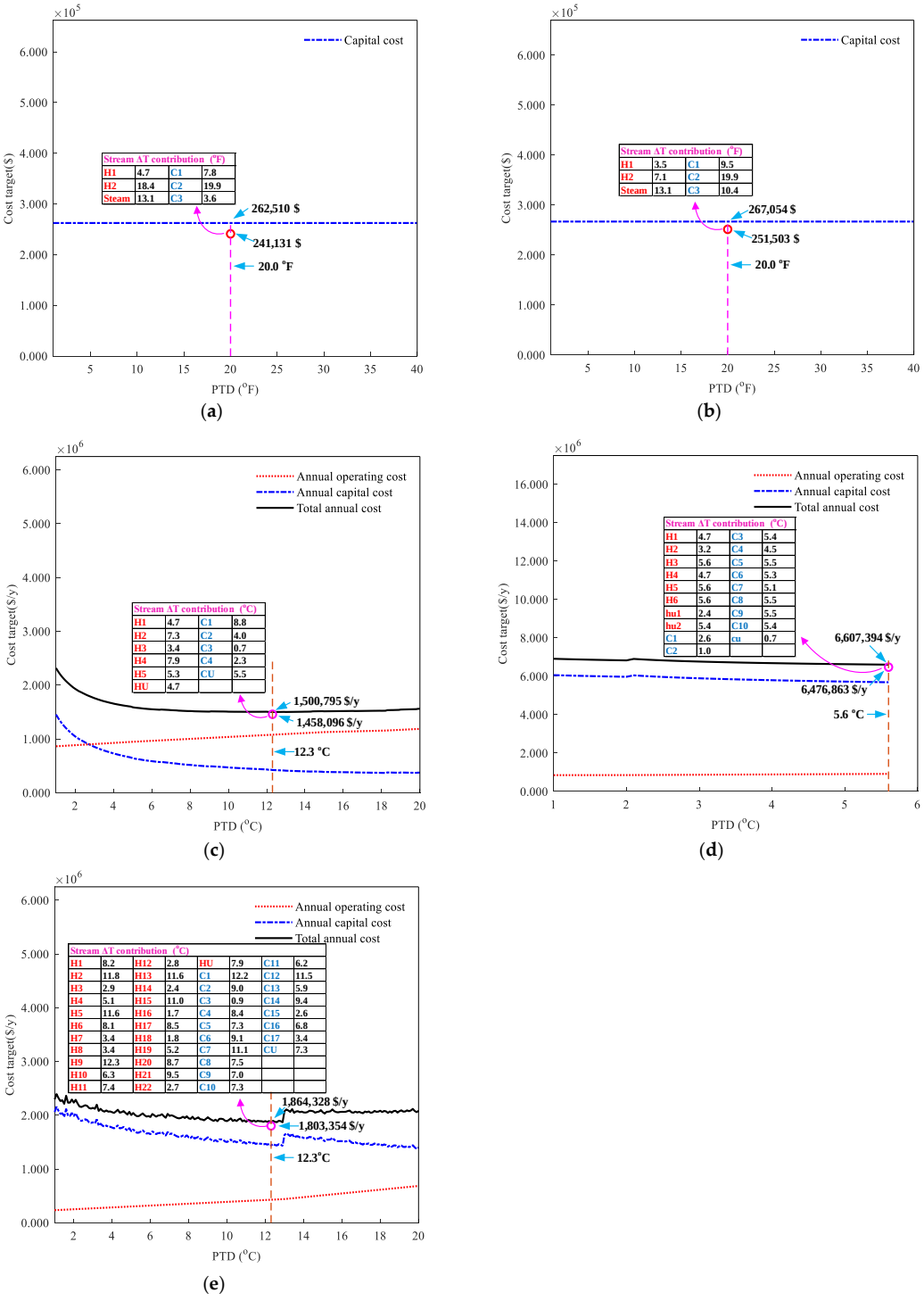

Figure 6. The optimal cost targets of HEN under the uniform and individual TDCs of streams; (**a**,**b**) contains situations without and with maximum area limitations for case study 1; (**c**) case study 2; (**d**) case study 3; (**e**) case study 4.

6.2. Case Study 2

The HEN of this case [25] also consisted of 1-2 shell and tube heat exchangers, but unlike case study 1, its HECC was type D. The HEN of this case had eleven streams. Using the uniform stream TDCs used for pinch analysis, Fu et al. [25] gave a total annual cost of 1,517,678 $/y by optimizing the TDFs of heat exchange matches. In comparison to the previous study results from Refs. [18,34], the 1,517,678 $/y shows the best total annual cost, which was appropriate to compare with the derived optimal total annual cost target. The case data and the target value derivation can be found in the Supplementary Material (Section S6.2). The target value obtained by optimizing the TDCs of stream is given in case 2 of Table 3.

The target deviations of total annual cost derived using optimal uniform and individual TDCs of streams were −1.1% and −3.9%, respectively. The deviation results indicate that by optimizing the individual TDCs of streams, the optimal total annual cost of HEN can be further reduced. Since the streams were constrained to using a common MTD of 11.1 °C in the optimization of Fu et al. [25], a deviation of −1.1% when under optimal uniform TDCs needed to be used. The absolute target deviation of total annual cost was within 5%.

6.3. Case Study 3

In this case [35], countercurrent heat exchangers were used in the HEN. Since there was no maximum area limitation for heat exchangers, the HECC could be considered type A or C. The HEN was a problem of nineteen streams. Many studies have been dedicated to obtaining the optimum HEN for this case (see Table 4). Pavão et al. [36] provided the lowest cost value. Their total annual cost of 6,712,551 $/y was most appropriate as the reference cost to evaluate the accuracy of the derived optimal total annual cost target. The case data and the target value derivation can be found in Supplementary Material S6.3. The target value obtained by optimizing the TDCs of stream is given in case 3 of Table 3.

Table 4. Various study results on the optimal total annual cost of HEN for case study 3.

Author	Ref.	Total Annual Cost ($/y)
Khorasany and Fesanghary (2009)	[37]	7,435,740
Huo Zhaoyi et al. (2013)	[38]	7,361,190
Pavão et al. (2017a)	[39]	7,301,437
Zhang et al. (2017)	[40]	7,212,115
Chen et al. (2017)	[41]	6,989,989
Zhang and Cui (2018)	[42]	6,861,111
Pavão et al. (2018)	[43]	6,801,261
Pavão et al. (2018)	[36]	6,712,551
Bao et al. (2018)	[44]	6,869,610
Xiao et al. (2019)	[45]	6,798,067
Kayange et al. (2020)	[35]	6,716,343

The target deviations of total annual cost under optimal uniform and individual TDCs were −1.6% and −3.5%, respectively. The deviation results indicate that using individual TDCs for streams has an obvious cost advantage compared to using uniform TDCs. Since the optimization method of Pavão et al. [36] did not impose a common MTD constraint, the −3.5% target deviation under optimal individual TDCs of streams needed to be used. The absolute target deviation of total annual cost based on the general ESPA method was within 5%.

6.4. Case Study 4

This is a case [5] in which the countercurrent heat exchangers were only applied in the HEN. The HECC is type A or C. Since there is no maximum area limitation, these two types of HECCs have the same cost calculation. A large-size HEN with forty-one streams is provided. For this case, there have been many attempts to obtain the optimum HEN, as

shown in Table 5. Xu et al. [5] provided the current lowest total annual cost of 1,852,723 $/y for the HEN, which was the most appropriate reference cost to compare with the optimal total annual cost target. The case data and the target value derivation can be found in Supplementary Material S6.4). The target value obtained by optimizing the TDCs of stream is given in case 4 of Table 3.

Table 5. Various study results on the optimal total annual cost of HEN for case study 4.

Author	Ref.	Total Annual Cost ($/y)
Björk and Pettersson (2003)	[46]	2,073,251
Pettersson (2005)	[47]	1,997,054
Luo et al. (2009)	[48]	1.965×10^6
Ernst et al. (2010)	[49]	1,943,536
Huang and Karimi (2014)	[50]	1,937,377
Zhang et al. (2016)	[51]	1,939,149
Pavão et al. (2017)	[52]	1,900,614
Xiao et al. (2018)	[53]	1,936,288
Nemet et al. (2019)	[54]	1.9288×10^6
Xiao et al. (2019)	[45]	1,925,783
Xiao et al. (2020)	[55]	1,921,639
Xiao et al. (2020)	[3]	1,873,813
Zhang et al. (2020)	[56]	1,918,593
Rathjens and Fieg (2020)	[6]	1,852,913
Xiao et al. (2021)	[8]	1,910,630
Xu et al. (2021)	[5]	1,852,723

The total annual cost target curve under uniform TDCs of stream shows a good cost change trend in Figure 6e. We noted that the total annual cost target curve was not smooth, originating from the slight fluctuation of the annual capital cost target curve. This phenomenon means that a small change to the TDC of stream can cause a perceptible fluctuation of capital cost target in this case study. This was further confirmed by changing the decimal position of the optimal individual TDCs of streams. When the decimal position was taken as one, the total annual cost target became 1,880,437 $/y, which is very different from the original 1,803,354 $/y.

The target deviation of total annual cost with optimal uniform TDCs used by streams was 0.6%. When optimal individual TDCs were used for streams, the target deviations of total annual cost under the original decimal place and one decimal place were −2.7% and 1.5%, respectively. The optimal individual TDCs of streams are more cost-effective than the optimal uniform TDCs of streams. Since the common MTD of streams was not imposed by Xu et al. [5] to optimize the HEN, either the target deviation of −2.7% or the target deviation of 1.5% under the optimal individual TDCs of stream needed to be used. No matter which target deviation was used, the absolute target deviation s within 5%. However, additional work should be done to handle the capital cost target fluctuations in this case study to obtain a more accurate target value.

6.5. Accuracy Enhancement Measures

There are two deficiencies in these case studies. One is in case study 1: without maximum area limitation, the capital cost target under optimal individual TDCs of streams was too low, reflected in the close to −10% deviation of this capital cost target from the optimal capital cost. The other is a fluctuation in the total annual cost target or capital cost target shown in case study 4. To address these two issues, target correction measure and a fluctuation coping measure were taken to improve the general ESPA method. For the first issue, following a thorough trade-off for all cases in the numerical experiments and case studies, a multiplier of 1.03 was used to correct the capital cost target, $CC_{HEN,mul}$, of HEN. The revised value $CC_{HEN,mul}$ was found as shown in Equation (44). The target deviation range of capital cost was then updated for all cases in numerical experiments to (−4.7%,

8.8%) (see Figure S8); thus, the absolute values were still within 10%. Figure S9 shows the re-optimized optimal cost target results for each case in the case studies. The target deviations were updated to −5.9% and −3.2 % for situations without and with maximum area limitations in case study 1, −0.3% for case study 2, −1.1% for case study 3, and −0.6% or 1.4% for case study 4. When the second issue occurs, just like the fluctuation of the capital target of HEN in case study 4, a method to provide a stable capital cost target should be adopted, as shown in Equation (45). One approximate solution set can be obtained by slightly changing the TDCs of streams in the optimal solution set by the same value. According to this approach, in case study 4, the stable total annual cost targets under the optimal uniform and individual TDCs of streams were 1,925,692 \$/y and 1,902,880 \$/y, respectively. The target deviations of total annual cost were 3.9% and 2.7%, accordingly. Based on the reason illustrated in case study 4, the target deviation of 2.7% under the optimal individual TDCs of stream was used. Figure 7 summarizes the calculation process of the general ESPA method.

$$CC_{\mathrm{HEN,mul}} = 1.03CC_{\mathrm{HEN}} \tag{44}$$

$$CC_{\mathrm{HEN,sta}} = \sum_{nt=1}^{21} CC_{\mathrm{HEN,mul}}(X_{\Delta \mathrm{T\_cont},nt})/21 \tag{45}$$

where

$$X_{\Delta \mathrm{T\_cont},nt} = \left[\Delta T_{\mathrm{cont},1},\ \Delta T_{\mathrm{cont},2},\ \ldots,\ \Delta T_{\mathrm{cont},I+J}\right] + ((nt-1) \times 0.005 - 0.05)$$

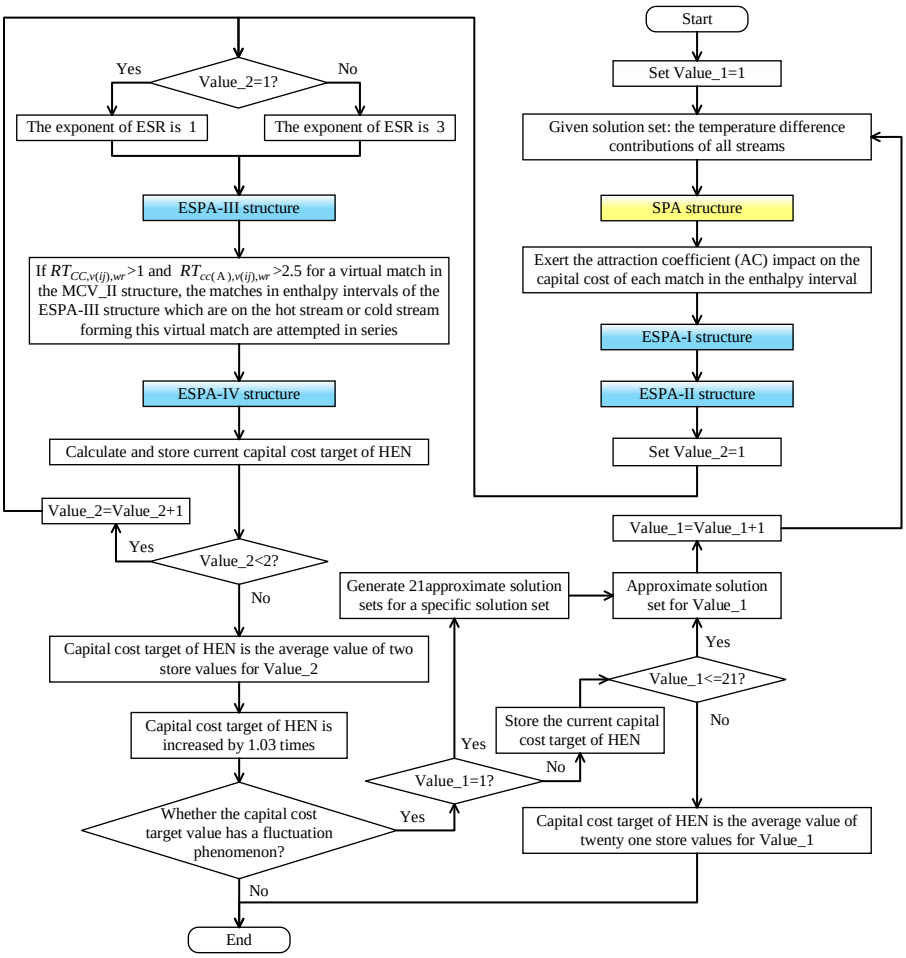

Figure 7. Calculation flowchart of the general ESPA method for capital cost target.

7. Discussion

7.1. Significance of Work

Pinch analysis has demonstrated its powerful energy recovery capacity when solving energy utilization problems. In order to determine good pinch positions that are cost-effective, the operating and capital cost targets need to be weighed before HEN design. Therefore, providing a reliable capital cost target for HEN is a step that should not be ignored. Although related studies have contributed to obtaining the capital cost target of HEN, a general targeting method is still lacking to suit the complex application scenarios in industries. We adopted the ESPA structure [25] to establish our targeting method but consider the generality issues to extend the targeting method's applicability.

The accuracy, robustness, and applicability of the provided general ESPA method under various case scenarios were demonstrated by comparing the related cost targets and reference costs. This capital-cost-targeting method can be used to determine the optimal pinch position required for pinch analysis and evaluate the design quality of HEN. The studied general ESPA method can further unlock the guiding power of pinch analysis in obtaining the HENs with the lowest cost consumption. The pursuit of the cost-effectiveness of HEN will help avoid wasting resources and promote sustainable development.

7.2. Limitations of Work

Although the provided targeting method was used to predict the optimal capital cost of HEN rather than give the design details of HEN, this study contributes to promoting the application effect of pinch analysis. The use of pinch analysis is straightforward and full of physical insights. However, it is critical to determine the target point for pinch analysis at the targeting stage. This work ensures the reliability of the optimal target point, thus providing a good starting point for the subsequent HEN design using pinch analysis.

The capital-cost-targeting method is a deterministic calculation approach, in which the target value can be quickly obtained after giving the TDCs of all streams. The trade-off for the energy and capital costs of the HEN is efficient. The targeting method presents complexity due to its expanded adaptability to application scenarios and enhanced accuracy during the method construction. In order to balance the problem of solving precision and calculation efficiency, it can be modified, simplified, and improved according to particular needs, for example, by searching for a new approach to loop elimination, simplifying the model for a specific scenario, and discarding some designs that ensure accuracy when facing the common process systems.

8. Conclusions

This paper provides a pinch-based general ESPA method to obtain the capital cost target of HEN. The ESPA structure was obtained by four loop elimination stages. The final ESPA structure oriented by the optimal matching distribution was generated as the base to derive the general ESPA method. To improve the accuracy and robustness of the method, four measures—the stability measure, accuracy measure, target correction measure, and fluctuation coping measure—were implemented, making this targeting method reliable. The main conclusions are as follows:

(1) The proposed targeting method has wide applicability. As required, this targeting method can flexibly impose area limitations, freely set HECCs for stream pairs, or apply non-uniform cost laws for a particular stream pair.
(2) The prediction capacity of the targeting method was enhanced. The use of individual stream TDCs is allowed for the targeting method, achieving more cost prediction possibilities. The effects of optimizing the individual stream TDCs are demonstrated in case studies.
(3) Excellent target accuracy is verified. The absolute deviations between capital cost targets and reference capital costs are less than 10% in all numerical experiments and often less than 5%. The absolute target deviations were the same in case studies where the best HEN cost results in the literature were used as references.

(4) The cost target derived by applying the general ESPA method can be used as a benchmark to guide the synthesis of HEN and evaluate the quality of the designed HEN. If the capital cost of HEN is 10% higher than the target value, the HEN synthesis is very likely to need improvement. Improving the designed HEN further would be difficult when the capital cost of HEN is close to the value of 10% lower than the target result.

The capital-cost-targeting method, due to its high accuracy, allows for a better trade-off between operating and capital costs at the targeting stage of pinch analysis, thus ensuring the economy of pinch analysis. In the future, the capital-cost-targeting method can be applied to more industrial practices to achieve substantial energy recovery with small capital costs.

Supplementary Materials: The following supporting information can be downloaded at https://www.mdpi.com/article/10.3390/pr11030923/s1. S1. Eliminating the loops formed by matches among different stream pairs. S2. The determination of the attraction coefficient. S3. The operation of parallel to serial. S4. Supporting content for accuracy test. S5. Supporting content for accuracy analysis. S6. Supporting content for case studies. S7. Supporting content for the target correction measure. Reference [57] are cited in the supplementary materials.

Author Contributions: D.F.: Conceptualization, Investigation, Methodology, Writing—original draft, Visualization. Q.L.: Validation, Writing—Review & Editing, Visualization. Y.L. (Yan Li): Validation, Writing—Review & Editing. Y.L. (Yanhua Lai): Conceptualization, Methodology, Supervision, Project Administration, Funding. L.L.: Formal Analysis, Methodology, Supervision, Validation, Funding. Z.D.: Supervision, Validation. M.L.: Supervision, Validation. All authors have read and agreed to the published version of the manuscript.

Funding: This research was funded by The Major Science and Technology Project of Inner Mongolia Autonomous Region (Grant No. 2021ZD0032), Program of Science and Technology of Suzhou (No. SS202137), and PolyU Joint Supervision Scheme with the Chinese Mainland, Taiwan and Macao Universities (P0039491).

Institutional Review Board Statement: Not applicable.

Informed Consent Statement: Not applicable.

Data Availability Statement: Not applicable.

Conflicts of Interest: The authors declare no conflict of interest.

Nomenclature

variables	
A	Area of heat exchange
CC	Capital cost
cc	Capital cost per unit energy or area
CP	Heat capacity flow rate
$D_{T/R}$	Capital cost target deviation
E	Indication of the existence of a match
F_{T}	LMTD correction factor
h	Heat transfer coefficient of the stream
N_{shell}	Number of shells in series
q	Heat exchange load between streams
RC	Reference cost
RT	Ratio value
ΔT_{LM}	Logarithmic mean temperature difference
parameters	
a, b, c	Cost parameters of heat exchanger specification
γ	Exponent of ESR

indexes	
C	Cold stream
cont	Contribution
H	Hot stream
i	Index of hot stream
ir	Independent region
j	Index of cold stream
k	Index of enthalpy interval
l	Index of heat exchanger specification
m	Heat exchange match
RC	Reference cost
se	Sub-cost law
TC	Target cost
U	Heat exchange unit
v	Virtual match
wr	Whole region
x	One certain segment of heat exchanger unit
z	Index of the enthalpy interval that forms a virtual match
abbreviations	
AC	Attraction coefficient
ATM	Automated targeting model
BCC	Balanced composite curve
ESR	Energy shift ratio
ESPA	Evolved from the spaghetti structure
GA	Genetic algorithm
HECC	Heat exchanger cost category
HEN	Heat exchanger network
LMTD	Logarithmic mean temperature difference
MTD	Minimum temperature difference
PTD	Pinch temperature difference
SIR	Structure identification and change of reference system
SPA	Spaghetti
TDC	Temperature difference contribution
TDF	Temperature driving force

References

1. Sun, X.; Zhuang, Y.; Liu, L.; Dong, Y.; Zhang, L.; Du, J. Multi-objective optimization of heat exchange network and thermodynamic cycles integrated system for cooling and power cogeneration. *Appl. Energy* **2022**, *321*, 119366. [CrossRef]
2. Fieg, G.; Luo, X.; Jezowski, J. A monogenetic algorithm for optimal design of large-scale heat exchanger networks. *Chem. Eng. Process. Process Intensif.* **2009**, *48*, 1506–1516. [CrossRef]
3. Xiao, Y.; Sun, T.; Cui, G. Enhancing strategy promoted by large step length for the structure optimization of heat exchanger networks. *Appl. Therm. Eng.* **2020**, *173*, 115199. [CrossRef]
4. Xiao, Y.; Cui, G.; Zhang, G.; Ai, L. Parallel optimization route promoted by accepting imperfect solutions for the global optimization of heat exchanger networks. *J. Cleaner Prod.* **2022**, *336*, 130354. [CrossRef]
5. Xu, Y.; Cui, G.; Han, X.; Xiao, Y.; Zhang, G. Optimization route arrangement: A new concept to achieve high efficiency and quality in heat exchanger network synthesis. *Int. J. Heat Mass Transfer* **2021**, *178*, 121622. [CrossRef]
6. Rathjens, M.; Fieg, G. A novel hybrid strategy for cost-optimal heat exchanger network synthesis suited for large-scale problems. *Appl. Therm. Eng.* **2020**, *167*, 114771. [CrossRef]
7. Feyli, B.; Soltani, H.; Hajimohammadi, R.; Fallahi-Samberan, M.; Eyvazzadeh, A. A reliable approach for heat exchanger networks synthesis with stream splitting by coupling genetic algorithm with modified quasi-linear programming method. *Chem. Eng. Sci.* **2022**, *248*, 117140. [CrossRef]
8. Xiao, Y.; Kayange, H.A.; Cui, G.; Li, W. Node dynamic adaptive non-structural model for efficient synthesis of heat exchanger networks. *J. Cleaner Prod.* **2021**, *296*, 126552. [CrossRef]
9. Bayomie, O.S.; Abdelaziz, O.Y.; Gadalla, M.A. Exceeding Pinch limits by process configuration of an existing modern crude oil distillation unit—A case study from refining industry. *J. Clean. Prod.* **2019**, *231*, 1050–1058. [CrossRef]
10. Bandyopadhyay, R.; Alkilde, O.F.; Upadhyayula, S. Applying pinch and exergy analysis for energy efficient design of diesel hydrotreating unit. *J. Clean. Prod.* **2019**, *232*, 337–349. [CrossRef]

11. Wang, M.; Deng, C.; Wang, Y.; Feng, X. Exergoeconomic performance comparison, selection and integration of industrial heat pumps for low grade waste heat recovery. *Energy Convers. Manage.* **2020**, *207*, 112532. [CrossRef]
12. Ghorbani, B.; Ebrahimi, A.; Rooholamini, S.; Ziabasharhagh, M. Pinch and exergy evaluation of Kalina/Rankine/gas/steam combined power cycles for tri-generation of power, cooling and hot water using liquefied natural gas regasification. *Energy Convers. Manage.* **2020**, *223*, 113328. [CrossRef]
13. Liu, S.; Yang, L.; Chen, B.; Yang, S.; Qian, Y. Comprehensive energy analysis and integration of coal-based MTO process. *Energy* **2021**, *214*, 119060. [CrossRef]
14. Langner, C.; Svensson, E.; Harvey, S. A computational tool for guiding retrofit projects of industrial heat recovery systems subject to variation in operating conditions. *Appl. Therm. Eng.* **2021**, *182*, 115648. [CrossRef]
15. Asante, N.D.K.; Zhu, X.X. An automated and interactive approach for heat exchanger network retrofit. *Chem. Eng. Res. Des.* **1997**, *75*, 349–360. [CrossRef]
16. Wang, B.; Klemeš, J.J.; Li, N.; Zeng, M.; Varbanov, P.S.; Liang, Y. Heat exchanger network retrofit with heat exchanger and material type selection: A review and a novel method. *Renew. Sustain. Energy Rev.* **2021**, *138*, 110479. [CrossRef]
17. Gundersen, T.; Grossmann, I.E. Improved optimization strategies for automated heat exchanger network synthesis through physical insights. *Comput. Chem. Eng.* **1990**, *14*, 925–944. [CrossRef]
18. Ahmad, S.; Linnhoff, B.; Smith, R. Cost optimum heat exchanger networks—2. Targets and design for detailed capital cost models. *Comput. Chem. Eng.* **1990**, *14*, 751–767. [CrossRef]
19. Jegede, F.O.; Polley, G.T. Capital cost targets for networks with non-uniform heat exchanger specifications. *Comput. Chem. Eng.* **1992**, *16*, 477–495. [CrossRef]
20. Serna-González, M.; Jiménez-Gutiérrez, A.; Ponce-Ortega, J.M. Targets for heat exchanger network synthesis with different heat transfer coefficients and non-uniform exchanger specifications. *Chem. Eng. Res. Des.* **2007**, *85*, 1447–1457. [CrossRef]
21. Akbarnia, M.; Amidpour, M.; Shadaram, A. A new approach in pinch technology considering piping costs in total cost targeting for heat exchanger network. *Chem. Eng. Res. Des.* **2009**, *87*, 357–365. [CrossRef]
22. Serna-González, M.; Ponce-Ortega, J.M. Total cost target for heat exchanger networks considering simultaneously pumping power and area effects. *Appl. Therm. Eng.* **2011**, *31*, 1964–1975. [CrossRef]
23. Diban, P.; Foo, D.C.Y. A pinch-based automated targeting technique for heating medium system. *Energy* **2019**, *166*, 193–212. [CrossRef]
24. Ulyev, L.; Boldyryev, S.; Kuznetsov, M. Investigation of process stream systems for targeting energy-capital trade-offs of a heat recovery network. *Energy* **2023**, *263*, 125954. [CrossRef]
25. Fu, D.; Nguyen, T.; Lai, Y.; Lin, L.; Dong, Z.; Lyu, M. Improved pinch-based method to calculate the capital cost target of heat exchanger network via evolving the spaghetti structure towards low-cost matching. *J. Cleaner Prod.* **2022**, *343*, 131022. [CrossRef]
26. Jiang, N.; Shelley, J.D.; Doyle, S.; Smith, R. Heat exchanger network retrofit with a fixed network structure. *Appl. Energy* **2014**, *127*, 25–33. [CrossRef]
27. Kemp, I.C. *Pinch Analysis and Process Integration: A User Guide on Process Integration for the Efficient Use of Energy*, 2nd ed.; Elsevier: Oxford, UK, 2007.
28. Jiang, N.; Bao, S.; Gao, Z. Heat Exchanger Network Integration Using Diverse Pinch Point and Mathematical Programming. *Chem. Eng. Technol.* **2011**, *34*, 985–990. [CrossRef]
29. Bowman, R.A.; Mueller, A.C.; Nagle, W.M. Mean temperature difference in design. *Trans. ASME* **1940**, *62*, 283–294. [CrossRef]
30. Smith, R. *Chemical Process Design and Integration*; Wiley: Chichester, UK, 2005; ISBN 0471486817.
31. Dehghani, M.J.; Yoo, C. Three-step modification and optimization of Kalina power-cooling cogeneration based on energy, pinch, and economics analyses. *Energy* **2020**, *205*, 118069. [CrossRef]
32. Galli, M.R.; Cerdá, J. Synthesis of heat exchanger networks featuring a minimum number of constrained-size shells of 1-2 type. *Appl. Therm. Eng.* **2000**, *20*, 1443–1467. [CrossRef]
33. Chauhan, S.S.; Khanam, S. Simultaneous water and energy conservation in non-isothermal processes—A case study of thermal power plant. *J. Clean. Prod.* **2021**, *282*, 125423. [CrossRef]
34. Ponce-Ortega, J.M.; Serna-González, M.; Jiménez-Gutiérrez, A. Synthesis of multipass heat exchanger networks using genetic algorithms. *Comput. Chem. Eng.* **2008**, *32*, 2320–2332. [CrossRef]
35. Kayange, H.A.; Cui, G.; Xu, Y.; Li, J.; Xiao, Y. Non-structural model for heat exchanger network synthesis allowing for stream splitting. *Energy* **2020**, *201*, 117461. [CrossRef]
36. Pavão, L.V.; Costa, C.B.B.; Ravagnani, M.A.S.S. A new stage-wise superstructure for heat exchanger network synthesis considering substages, sub-splits and cross flows. *Appl. Therm. Eng.* **2018**, *143*, 719–735. [CrossRef]
37. Khorasany, R.M.; Fesanghary, M. A novel approach for synthesis of cost-optimal heat exchanger networks. *Comput. Chem. Eng.* **2009**, *33*, 1363–1370. [CrossRef]
38. Zhaoyi, H.; Liang, Z.; Hongchao, Y.; Jianxiong, Y. Simultaneous synthesis of structural-constrained heat exchanger networks with and without stream splits. *Can. J. Chem. Eng.* **2013**, *91*, 830–842. [CrossRef]
39. Pavão, L.V.; Costa, C.B.B.; Ravagnani, M.A.S.S. Heat Exchanger Network Synthesis without stream splits using parallelized and simplified simulated Annealing and Particle Swarm Optimization. *Chem. Eng. Sci.* **2017**, *158*, 96–107. [CrossRef]
40. Zhang, H.; Cui, G.; Xiao, Y.; Chen, J. A novel simultaneous optimization model with efficient stream arrangement for heat exchanger network synthesis. *Appl. Therm. Eng.* **2017**, *110*, 1659–1673. [CrossRef]

41. Chen, J.; Cui, G.; Duan, H. Multipopulation differential evolution algorithm based on the opposition-based learning for heat exchanger network synthesis. *Numeri. Heat Transf. A Appl.* **2017**, *72*, 126–140. [CrossRef]
42. Zhang, H.; Cui, G. Optimal heat exchanger network synthesis based on improved cuckoo search via Levy flights. *Chem. Eng. Res. Des.* **2018**, *134*, 62–79. [CrossRef]
43. Pavão, L.V.; Costa, C.B.B.; Ravagnani, M.A.S.S. An Enhanced Stage-wise Superstructure for Heat Exchanger Networks Synthesis with New Options for Heaters and Coolers Placement. *Ind. Eng. Chem. Res.* **2018**, *57*, 2560–2573. [CrossRef]
44. Bao, Z.; Cui, G.; Chen, J.; Sun, T.; Xiao, Y. A novel random walk algorithm with compulsive evolution combined with an optimum-protection strategy for heat exchanger network synthesis. *Energy* **2018**, *152*, 694–708. [CrossRef]
45. Xiao, Y.; Kayange, H.A.; Cui, G.; Chen, J. Non-structural model of heat exchanger network: Modeling and optimization. *Int. J. Heat Mass Transfer* **2019**, *140*, 752–766. [CrossRef]
46. Björk, K.-M.; Pettersson, F. Optimization of large-scale heat exchanger network synthesis problems. *Modell. Simul.* **2003**, *2003*, 313–318.
47. Pettersson, F. Synthesis of large-scale heat exchanger networks using a sequential match reduction approach. *Comput. Chem. Eng.* **2005**, *29*, 993–1007. [CrossRef]
48. Luo, X.; Fieg, G.; Cai, K.; Guan, X. Synthesis of Large-Scale Heat Exchanger Networks by a Monogenetic Algorithm. In *10th International Symposium on Process Systems Engineering: Part A*; Elsevier: Amsterdam, The Netherlands, 2009; ISBN 9780444534729.
49. Ernst, P.; Fieg, G.; Luo, X. Efficient synthesis of large-scale heat exchanger networks using monogenetic algorithm. *Heat Mass Transfer* **2010**, *46*, 1087–1096. [CrossRef]
50. Huang, K.F.; Karimi, I.A. Efficient algorithm for simultaneous synthesis of heat exchanger networks. *Chem. Eng. Sci.* **2014**, *105*, 53–68. [CrossRef]
51. Zhang, C.; Cui, G.; Chen, S. An efficient method based on the uniformity principle for synthesis of large-scale heat exchanger networks. *Appl. Therm. Eng.* **2016**, *107*, 565–574. [CrossRef]
52. Pavão, L.V.; Costa, C.B.B.; Ravagnani, M.A.D.S.S.; Jiménez, L. Large-Scale Heat Exchanger Networks Synthesis Using Simulated Annealing and the Novel Rocket Fireworks Optimization. *AlChE J.* **2017**, *63*, 1582–1601. [CrossRef]
53. Xiao, Y.; Cui, G.; Sun, T.; Chen, J. An integrated random walk algorithm with compulsive evolution and fine-search strategy for heat exchanger network synthesis. *Appl. Therm. Eng.* **2018**, *128*, 861–876. [CrossRef]
54. Nemet, A.; Isafiade, A.J.; Klemeš, J.J.; Kravanja, Z. Two-step MILP/MINLP approach for the synthesis of large-scale HENs. *Chem. Eng. Sci.* **2019**, *197*, 432–448. [CrossRef]
55. Xiao, Y.; Kayange, H.A.; Cui, G. Heat integration of energy system using an integrated node-wise non-structural model with uniform distribution strategy. *Int. J. Heat Mass Transf.* **2020**, *152*, 119497. [CrossRef]
56. Zhang, H.; Huang, X.; Peng, F.; Cui, G.; Huang, T. A novel two-step synthesis method with weakening strategy for solving large-scale heat exchanger networks. *J. Clean. Prod.* **2020**, *275*, 123103. [CrossRef]
57. Smith, R.; Jobson, M.; Chen, L. Recent development in the retrofit of heat exchanger networks. *Appl. Therm. Eng.* **2010**, *30*, 2281–2289. [CrossRef]